

Development of Medical Images Series Segmentation Technique Using Active Contours Models

*Prof. Dr. Abdul Monem S. Rahma * I. A. Alwan **

Abstract

Image segmentation, is one of the most important problems in computer vision and image processing. As a high-level technique for boundary identification, active contours are used extensively for segmentation purposes. Active contours or Snakes are curves defined in the image domain that can move under the influence of internal forces within the curve itself and external forces derived from the image data. In this research the Gradient Vector Flow (GVF snake) was used for the segmentation of brain tumor images. We used Magnetic Resonance image (MRI) dataset for our experiments. The results show that GVF snake is one of the most effective solutions for the problems of the traditional model of active contours. GVF provides a good capture rang and a good convergence; there fore; Good results are obtained; where GVF snake could successfully segment the brain tumor regions from MRI images.

*University of Technology, Department of Computer Science

1. Introduction

Automated detection of tumors in different medical images is motivated by the necessity of high accuracy when we are dealing with a *human life*. Also, the computer assistance is demanded in medical institutions due to the fact that it could improve the results of humans in such a domain where the false negative cases must be at a very low rate. It has been proven that double reading of medical images could lead to better tumor detection. But the cost implied in double reading is very high, on the other hand; the world goes to satisfy the health by following the prophylactic procedure (irrotational examinations), that's why good software to assist humans in medical institutions is of great interest nowadays.

2. Active Contours

Traditional snake is a curve $\mathbf{x}(s) = [x(s), y(s)]$ $s \in [0, 1]$ that moves through the spatial domain of an image to minimize the energy functional:

$$E = \int_0^1 \left[\frac{\alpha}{2} |\mathbf{x}'(s)|^2 + \beta |\mathbf{x}''(s)|^2 \right] + E_{\text{ext}}(\mathbf{x}(s)) ds \quad \dots (1)$$

Where α and β are weighting parameters that control the snake's tension and rigidity, respectively, $\mathbf{x}'(s)$ and $\mathbf{x}''(s)$ denote the first and second derivatives of $\mathbf{x}(s)$ with respect to s .

is derived from the image I_{ext} . The external energy function E so that it takes on its smaller values at the features of interest, such as boundaries. Given a gray-level image $I(x, y)$, viewed as a function of continuous position variables (x, y) , typical external energy designed to lead an active contour toward step edges is:

$$E_{\text{ext}}(x, y) = -\left| \nabla \left[G_{\sigma}(x, y) * I(x, y) \right] \right|^2 \quad \dots (2)$$

Where $G_{\sigma}(x, y)$ is a two-dimensional Gaussian function with standard deviation σ and ∇ is the gradient operator. Larger σ 's will cause the boundaries to become blurry. Such large σ 's are often necessary, however, in order to increase the capture range of the active contour. A snake that minimizes E must satisfy the Euler equation:

$$\alpha X''(s) - \beta X''''(s) - \nabla E_{\text{ext}} = 0 \quad \dots (3)$$

This can be viewed as a force balance equation:

$$F_{\text{int}} + F_{\text{ext}} = 0 \quad \dots (4)$$

Where $F_{\text{int}} = \alpha X''(s) - \beta X''''(s)$ and $F_{\text{ext}} = -\nabla E_{\text{ext}}$. The internal force F_{int} discourages stretching and bending while the external potential force F_{ext} pulls the snake toward the desired image edges.

To find a solution to (3), the snake is made dynamic by treating x as function of time t as well as S (i.e., $x(s, t)$). Then, the partial derivative of x with respect to t is then set equal to the left side of (3) as follows:

$$x_t(s, t) = \alpha X''(s, t) - \beta X''''(s, t) - \nabla E_{\text{ext}} \quad \dots (5)$$

When the solution $x(s, t)$ stabilizes, the term $x_t(s, t)$ vanishes and we achieve a solution of (3) [1]. A solution to (5) can be found by discretizing the equation and solving the discrete system iteratively. But the traditional snake has two limitations. First, the poor convergence. Specifically, concavities in the object of interest are rarely covered; i.e. the snake does not extend to the concave regions of the object. An example of that is shown in Fig (1). The second problem with snakes is the limited capture range, which is related to the initialization of the snake around the object of interest. The magnitude of external forces dies out far away from the boundaries. The technique presented by Xu and Prince in (1998) [2] addresses these issues and presents a new formulation for active contour modeling called the Gradient Vector Field or GVF snake [3, 4, 5]. They replaced the external potential force $-\nabla E_{\text{ext}}$ in (5) with v yields the following equation:

$$x_t(s, t) = ax''(s, t) - \beta x''''(s, t) + v \quad \dots (6)$$

3. GVF Snake Formation

The process starts by calculating the edge map of the given image, using any edge finding algorithm from the image processing literature.

$$f(x, y) = -E_{\text{ext}}(x, y) \quad \dots (7)$$

The edge map has three important features relating to snake formation. One, the gradient of this edge map ∇f has vectors pointing towards the edge, which is a desirable property for snakes.

Two, these vectors have large magnitude at the vicinity of the edges. Three, in homogenous regions (regions with little variation in image intensity) ∇f is almost zero, and therefore no information about nearby or distant edges is available.

The second and third features can be problematic when constructing an active contour. To keep the first feature and nullify the effect of the latter two, the gradient map is extended farther away from the edges and into homogenous regions using a computational diffusion process.

The gradient vector flow field is defined as the vector field $v(x, y) = (u(x, y), v(x, y))$ that minimizes the following energy functional:

$$\varepsilon = \int \int \mu (u_x^2 + u_y^2 + v_x^2 + v_y^2) + |\nabla f|^2 |v - \nabla f|^2 \, dx \, dy \quad \dots (8)$$

As can be seen, this is an example of variational formulation of regularization. The parameter μ is a regularizing parameter, which adjusts the tradeoff between the first and second terms of the integrand and is set according to the level of noise present in the image. Also, when the value of the edge gradient $|\nabla f|$ is small, energy is dominated by the sum of the partial derivatives of the gradient field, and yields a smooth field. On the other hand, when $|\nabla f|$ is large, the second term dominates the integrand. In this case, setting $v = \nabla f$ minimizes the energy. Overall, this formulation transforms the gradient

vector flow field by keeping it equal to the edge gradient at the boundaries; it also keeps v slowly varying at the homogenous regions of the image. Using the calculus of variations, it can be shown that the GVF field can be found by solving the pair of Euler equations.

$$m\nabla^2 u - (u - f_x)(f_x^2 + f_y^2) = 0 \quad \dots (9a)$$

$$m\nabla^2 v - (v - f_y)(f_x^2 + f_y^2) = 0 \quad \dots (9b)$$

Here, ∇^2 is the Laplacian operator. These equations give us another intuition behind the GVF formulation. It is noted that in homogeneous regions, the second term of both equations (9a) and (9b) is zero (because the gradient of $f(x, y)$ is zero).

Therefore, within these regions, u and v are each determined by Laplace's equation. This results in a type of "filling-in" of information taken from the boundaries of the region.

Equations (9a) and (9b) can be solved numerically by treating u and v as a function of time. The resulting equations are:

$$u_t(x, y, t) = \mu \nabla^2 u(x, y, t) - (u(x, y, t) - f_x(x, y)) \cdot (f_x^2(x, y) + f_y^2(x, y)) \quad \dots (10 a)$$

$$v_t(x, y, t) = \mu \nabla^2 v(x, y, t) - (v(x, y, t) - f_y(x, y)) \cdot (f_x^2(x, y) + f_y^2(x, y)) \quad \dots (10 b)$$

The steady-state solution of equation (10a) and (10b) yields the solution to the Euler equations (9a) and (9b). An iterative solution can be set up for solving the equations above [2]; see Fig (2).

Equations in (10a, 10b) are known as *generalized diffusion equations*, and are known to arise in such diverse fields as heat conduction, reactor physics, and fluid flow [6]. In GVF snake, they are used to satisfy “filling in” property.

4. Numerical Methods for GVF Fields

Here, numerical methods are described for computing GVF fields.

- GVF field is obtained by solving Euler equations; and these equations can be solved by treating u and v as function of time:

$$u_t(x, y, t) = m \nabla^2 u(x, y, t) - [u(x, y, t) - k_x(x, y)] \cdot \left[k_x(x, y)^2 + k_y(x, y)^2 \right] \dots (11a)$$

$$v_t(x, y, t) = m \nabla^2 v(x, y, t) - [v(x, y, t) - k_y(x, y)] \cdot \left[k_x(x, y)^2 + k_y(x, y)^2 \right] \dots (11b)$$

- For convenience, the equations can be rewritten as follows:

$$u_t(x, y, t) = m \nabla^2 u(x, y, t) - b(x, y) u(x, y, t) + c^1(x, y) \dots (12a)$$

$$v_t(x, y, t) = m \nabla^2 v(x, y, t) - b(x, y) v(x, y, t) + c^2(x, y) \dots (12b)$$

Where

$$b(x, y) = k_x(x, y)^2 + k_y(x, y)^2$$

$$c^1(x, y) = b(x, y) k_x(x, y)$$

$$c^2(x, y) = b(x, y) k_y(x, y)$$

- To set up the iterative solution, let the indices i, j and n correspond to x, y and t , respectively, and let the spacing between pixels be Δx and Δy and the time step for each iteration be Δt . Then the required partial derivatives can be approximated as:

$$u_t = \frac{1}{\Delta t} (u_{i,j}^{n+1} - u_{i,j}^n) \dots (13)$$

$$v_t = \frac{1}{\Delta t} (v_{i,j}^{n+1} - v_{i,j}^n) \dots (14)$$

$$\nabla^2 u = \frac{1}{\Delta x \Delta y} (u_{i+1,j} + u_{i,j+1} + u_{i-1,j} + u_{i,j-1} - 4u_{i,j}) \dots (15)$$

$$\nabla^2 v = \frac{1}{\Delta x \Delta y} (v_{i+1,j} + v_{i,j+1} + v_{i-1,j} + v_{i,j-1} - 4v_{i,j}) \dots (16)$$

- Substituting these approximation into equations gives our iterative solution to GVF as follows:

$$\begin{aligned}
 u_{i,j}^{n+1} &= (1 - b_{i,j} \Delta t) u_{i,j}^n \\
 &\quad - \tau (u_{i+1,j}^n + u_{i,j+1}^n + u_{i-1,j}^n + u_{i,j-1}^n - 4u_{i,j}^n) \\
 &\quad + c_{i,j}^n \Delta t \dots (17a)
 \end{aligned}$$

$$\begin{aligned}
 v_{i,j}^{n+1} &= (1 - b_{i,j} \Delta t) v_{i,j}^n \\
 &\quad + \tau (v_{i+1,j}^n + v_{i,j+1}^n + v_{i-1,j}^n + v_{i,j-1}^n - 4v_{i,j}^n) \\
 &\quad + c_{i,j}^n \Delta t \dots (17b)
 \end{aligned}$$

5. GVF Snake Algorithm

Algorithm of GVF snake is shown in the Fig (3), and the algorithm that finds GVF force field is shown in the Fig (4).

6. Implementation of GVF Snake

First, the GVF snake algorithm was implemented on a line drawing U-shape image so to see the important differences in performance between the traditional snake algorithm and GVF snake algorithm. The parameters that should be given are m and no. of iteration for (GVF field), and a , b and no. of iteration for (GVF snake); and their values are shown in the table (1). See Fig (5). Because of the good results that were obtained from GVF snake implementation on U-shape image, it can be used to segment the brain tumor from MRI images. GVF snake algorithm was implemented on two cases, one of a patient man who was 62 years old. He suffered from brain tumor; called (*Adenocarcinoma*) and the second case is a woman who is 42 years old that suffers from brain tumor called (*Bronchogenic Carcinoma*). The parameters' values of two cases are shown in table (2). See Fig (6) and Fig (7).

Note: MRI Images of patients' cases are taken from the Whole Brain Atlas of School Medicine of Harvard University [7].

7. Application to Multiple Slices

The Graphical User Interface (GUI) of the program has the ability to save the current snake, and to then reload it for use on the same image or other images. Therefore, the snake can be applied and iterated on a slice from a dataset

and when the segmentation of a region of interest is completed, by opening the next slice and loading this snake, the snake will appear at the same coordinate positions as in the previous slice, and it can then be iterated on the new slice. Hence, no snake initialization is required for the second slice. This results in time saving and simplicity of operation. Fig (8) illustrates this feature of GUI on four successive slices of an MRI dataset. An initial snake is implemented and iterated to segment a desired structure in a slice (i.e., slice 04), and the converged snake is loaded on the successive slice (i.e., 05), for the same structure.

Thereafter, by iterating the snake on this slice, it fits itself to the boundary of the structure in this slice and segments the desired structure. This example continues this process on the next slice (i.e., 07).

In Fig (8), (a) is the initial snake (in red color) on slice 04 of MRI dataset, (b) the final snake (in green color) after 10 iterations when the snake converges to the boundary, (c) the snake (in green color) loaded on the same structure in slice 05, (d) the final snake on slice 05 after 10 iterations, (e) the snake loaded on the same structure in slice 06, and (f) the final snake on slice 06 after 10 iterations. (g) the snake loaded on the same structure in slice 07, and (h) the final snake on slice 07 after 10 iterations. The values of parameters of each slice in the series of a same case may not be similar, for example the no. of iteration in first slice may be 20 and the second slice may be 100.

8. Conclusion

It is found that the generic segmentation algorithms (thresholding approaches, region-based approaches, edge-based approaches) are usually easy to use. However, they are all sensitive to noise. They tend to over segment the images. Moreover, the segmentation results may not correspond to the desired object. *They failed with the medical images because of the sheer size of data sets and the complexity and variability of the anatomic shapes of interest.*

The Active Contour Models (Snakes) are the popular approaches currently used in medical image segmentation. The traditional model of active contour was sensitive to the initial configurations of the contours and wasn't able to deal with topological changes on the snake contour. The GVF snake of Xu and Prince solved the problems of the traditional model by extending the gradient map farther away from the edges and into homogeneous regions using computational diffusion process. The efficiency of snakes depends on a set of parameters such as alpha (elasticity parameter), beta (rigidity parameter), iteration no. etc. when the user gives the appropriate values, the snake deforms well and locks on the desired object. Also it is found that, there is no way to compute or directly give the appropriate values for these parameters, but by experiments and common sense; with respect to our experiments we found that the acceptable range for each parameter is as follows: Increasing β will increase the rigidity of the model and would affect the shape even if close to start with. We found that the rigidity parameter can be increased from 0 to 0.03 with almost the same results.

Decreasing the tension parameter causes the active contour to follow the influence of the external force and lose its smoothness.

The acceptable range that we found for tension was from 0.02 to 0.08. For values over $\alpha = 0.08$, the active contour must be initialized close to the boundary; otherwise, the tension force tries to contract the model and prevents the contour points from easily converging to the boundary.

The acceptable range for m , it was from 0 to 0.2, but if the desired object has sharp corners the value of m must be less than 0.1 else the final configuration has slightly rounder corners. The appropriate number of iterations for computing GVF was 80 iterations.

Also it is found that the best combination of the parameters may vary depending on the characteristics of the region of interest (i.e., the contrast and shape), the number of points of the initial contour, and the distance of the points from the boundary.

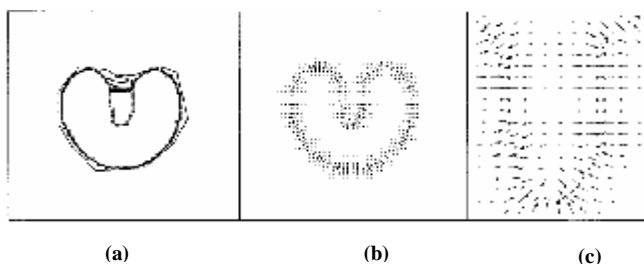


Fig (1): (a) Convergence of a snake (b) traditional potential forces, and (c) shown close-up the boundary concavity

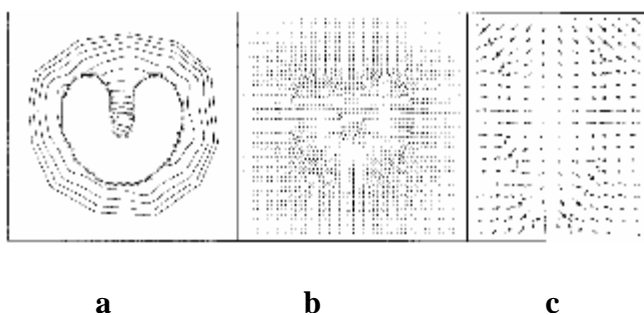


Fig (2): (a) Convergence of a snake (b) GVF external forces, and (c) shown close-up within the boundary concavity

Input: MRI image of brain tumor, the control points of the GVF snake.

Output: Final GVF snake locked on brain tumor in the MRI image.

Begin

Step1: If the objects of interest are present like line-like structures in the image, the input image can be directly used as the edge map.

Step2: If the objects are present as homogenous regions whose boundaries separate the regions from the background of different intensity value, an edge map has to be computed.

Step3: If required, normalize the edge map to have all edge intensities fall between 0 and 1.

Step4: Input the normalized edge map to *GVF Solver*. This will produce the GVF field of edge map.

Step5: The GVF snake can be formed by following the direction of the gradient field vectors over a certain number of iterations until a statistical equilibrium is reached.

End

Fig (3): GVF snake algorithm

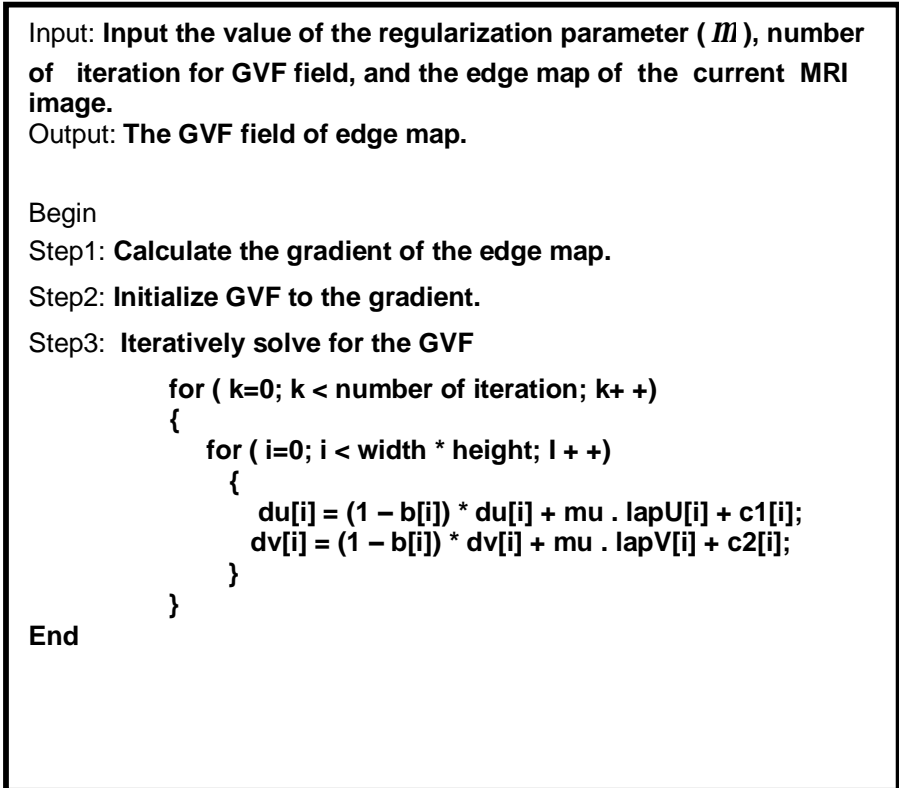


Fig (4): GVF solver algorithm

Mu (μ)	Iteration No. for GVF field	Alpha (α)	Beta (β)	Iteration No. for GVF snake
0.2	80	0.05	0	80

Table (1): Values of GVF snake parameters with U-shape image

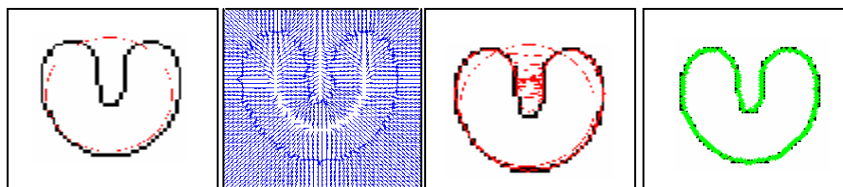


Fig (5): A snake with GVF external forces moves into the concave boundary region, (a) is the initial snake in red color, (b) GVF forces field, (c) is the snake deformation in red color, and (d) is the final snake in green color

Type of brain tumor	μ	α	Iteration No. for GVF field	β	γ	Iteration No. for GVF snake
Adenocarcinoma	3	0.2	80	0.09	0	10
Bronchogenic	2.5	0.2	80	0.05	0	200

Table (2): Values of GVF snake parameters with two patients' cases

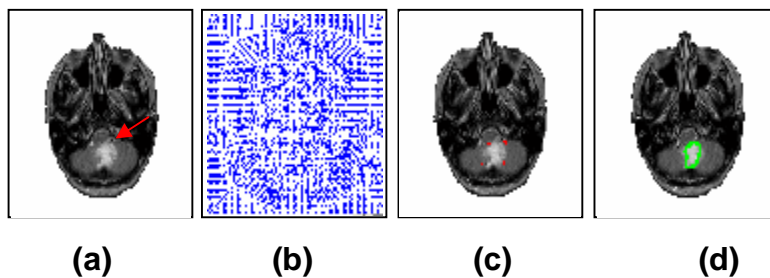


Fig (6): Segmenting brain tumor (Adenocarcinoma) by using GVF snake algorithm, (a) is the original image, (b) GVF forces field, (c) is the initial snake in red color, and (d) is the final snake in green color

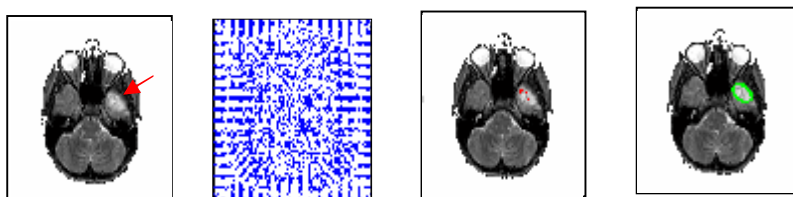


Fig (7): Segmenting brain tumor (Bronchogenic Carcinoma) by using GVF snake algorithm, (a) is the original image, (b) GVF forces field, (c) is the initial snake in red color, and (d) is the final snake in green color

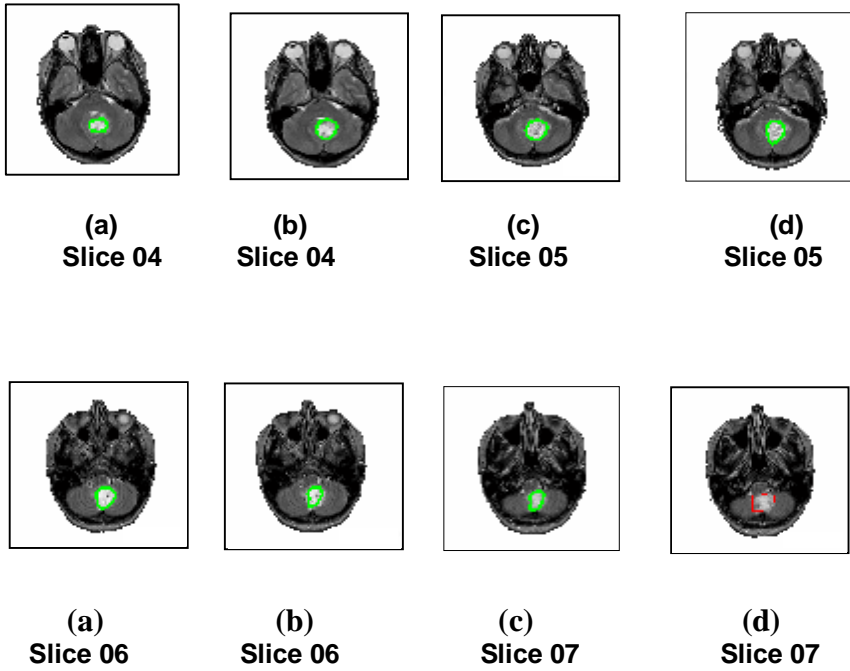


Fig (8): Example of the multi-loading property of active contours in GUI

Reference

1. Kass M., Witkin A., and Terzopoulos D., "*Snakes: active contour models*", International Journal of Computer Vision, 3, Pages 321-331, 1986.
2. Xu C. and Prince J. L., "*Snakes, shapes, and gradient vector flow*", IEEE Trans. On Image Processing, vol. 7, No. 3, Mar. 1998.
3. Derraz F., Beladgham M., and Khelif M., "*Application of active contour models in medical image segmentation*", IEEE Trans. On Information Technology: Coding and Computing, Department of Computer Science, Abou Bekr Belkaid University, Tlemcen, 2004.
4. Xu C., Yezzi Jr. A., and Prince J. L., "*On the relationship between parametric and geometric active contours*", Center for Imaging Science, Johns Hopkins University, Baltimore, 2000.
5. Xu C., Pham D. L., and Prince J. L., *Image Segmentation Using Deformable Models*, Handbook of Medical Imaging, Vol. 2, Medical Image Processing and Analysis, SPIE Press. , 2000.
6. Charles A. H. and Porsching T. A., "*Numerical analysis of partial differential equations*", Prentice Hall, Englewood Cliffs, NJ, 1990.
7. "The whole brain atlas", Medical School, Harvard University, Available at:
[http:// www.med.harvard.edu/ANNLIB/](http://www.med.harvard.edu/ANNLIB/)

تطوير تقنيه لتقطيع سلاسل الصور الطبيه بأستخدام نماذج المنحنيات النشيطة

اسراء عبد الجبار علوان *

أ.د. عبد المنعم صالح رحمة*

المستخلص

تقطيع الصورة، أحد أهم المشاكل في رؤية الحاسوب ومعالجة الصورة الرقميـة . كتقنية عالية المستوى لأستخلاص الحدود ، تم أستعمال المنحنيات النشيطة (Active Contour) على نطاق واسع لأغراض التقطيع. المنحنيات النشيطة هي عبارة عن خطوط منحنية تُعرف في مجال الصورة وتتحرك تحت تأثير قوى داخلية تُشتق من المنحنى نفسه وقوى خارجية تُشتق من بيانات الصورة. بالنسبة لتجارب هذا البحث ولغرض تقطيع اورام الدماغ من الصور فإنه تم استعمال الافةى العاملة وفقاً لتدفق متجهات الميل **GVF snake** , أما نوع الصور الطبيه المستعمله فهي سلسلة الصور الملتقطه بواسطة التصوير بالرنين المغناطيسي (MRI) . أظهرت نتائج هذا البحث بأن إحدى الحلول الأكثر فاعلية لمشاكل الافةى التقليديه هي الافةى العاملة وفقاً لتدفق متجهات الميل (**GVF snake**) حيث أنها تمتلك مدى التقاط كبير جداً كذلك يمكنها التكيف للتغيرات التبولوجيه, لذلك تم الحصول على نتائج جيده, حيث تمكنت الافةى العاملة وفقاً لتدفق متجهات الميل من تقطيع مناطق اورام الدماغ بنجاح من سلسلة الصور الملتقطه بواسطة التصوير بالرنين المغناطيسي.

*

الجامعه التكنولوجيه, قسم علم الحاسبات ونظم المعلومات